Towards a Modular Brain-Machine Interface for Intelligent Vehicle Systems Control – A CARLA Demonstration

Conference Paper · October 2019

DOI: 10.1109/SMC.2019.8914317

16 authors, including:

Dimitar Filev
Ford Motor Company
308 PUBLICATIONS **11,870** CITATIONS
SEE PROFILE

Marcia Bockbrader
BEP Medical Group LLC
81 PUBLICATIONS **1,520** CITATIONS
SEE PROFILE

Patrick Ganzer
University of Miami
25 PUBLICATIONS **431** CITATIONS
SEE PROFILE

Gaurav Sharma
Air Force Research Laboratory
69 PUBLICATIONS **2,021** CITATIONS
SEE PROFILE

Towards a Modular Brain-Machine Interface for Intelligent Vehicle Systems Control – A CARLA Demonstration*

Collin Dunlap, Luke Bird, Ian Burkhart, Kaitlyn Eipel, Samuel Colachis IV, Nicholas Annetta, Patrick Ganzer, Gaurav Sharma, David Friedenberg, Robert Franklin, Marcus Gerhardt, Aniruddh Ravindran, Ali Hassani, Dimitar Filev, *Member, IEEE*, Florian Solzbacher, *Senior Member, IEEE*, Marcia Bockbrader, *Member, IEEE*

***Abstract*—*Objective:* Individuals with paralysis often have mobility and dexterity impairments that limit their ability to operate motor vehicle controls. Integrating brain-machine interface (BMI) neurotechnology with vehicle control systems (VCS) provides a novel solution to this problem. In this proof-of-concept study, we show that an intracortical BMI developed to restore voluntary grasp can be repurposed to decode motor intention for vehicle velocity and steering control. *Methods:* The BMI-VCS consists of four components: 1) implanted motor cortex microelectrode array and NeuroPort data acquisition system, 2) machine learning workstation, 3) Python interface to generate control signals, and 4) vehicle control system. *Results:* Direct cortical steering and velocity control were achieved through accurate decoding of movement intention (supination, pronation, hand open, hand close) from the participant's motor cortex, translating intention into vehicle commands (turn right, turn left, accelerate, decelerate, respectively), and dynamically switching between commands to turn corners, start and stop, shift from forward to reverse, and parallel park. *Conclusion:* By translating BMI decoder outputs into high-level vehicle commands, a participant with tetraparesis from C5 ASIA A spinal cord injury successfully navigated CARLA driving simulator courses in real time. These decoder outputs could also be used offline for shared control of a scale model car. *Significance:* High-level, shared vehicle control with BMI-VCS offers an innovative way to return independent driving abilities to those with disability. BMI systems that can control multiple end-effectors may be particularly useful to those with paralysis.**

***Index Terms*—Assistive technology, brain-machine interface, steering control, velocity control, intelligent vehicle systems**

I. Introduction

People living with conditions that severely limit motor function face many challenges in tasks ranging from activities of daily living to mobility and leisure activities. Brain machine interfaces (BMIs) have been proposed as assistive devices to restore or replace lost functionality by interpreting neural activity to control effector devices. Proof of concept BMI systems have been demonstrated that enable humans with motor impairments to control a robotic arm [1, 2], computer cursor [3-5], wheelchair [6, 7], or their own paralyzed limbs through electrical stimulation (Estim) [8-12].

These BMI systems have historically been conceptualized as dedicated systems for a single set of related functions, e.g., to regain grasp. However, surveys reveal that potential BMI end-users value device multi-functionality, prioritizing both restoration of grasp and ability to control mobility devices, e.g., a powered wheelchair or car [13, 14]. In this report, we extend prior work using BMI to control Estim for hand grasp to show how the modular, intracortical BMI system can also provide high-level commands for shared control of driving. Shared control enables the user to provide high-level commands, such as intended vehicle speed, while low-level functions, such as acceleration, are left to intelligent vehicle control systems. We provide details of the BMI architecture, decoding algorithms, and training, then describe its integration with CARLA[15], an Unreal engine-based, open-source simulator for autonomous driving research. Next we show ability to navigate predetermined CARLA maps. Finally, to demonstrate that BMI outputs can be sent wirelessly to provide shared control of a physical vehicle, we used real-time decoders obtained during driving simulation to provide offline, high-level, remote control of a 1:10 scale Ford GT. This work demonstrates a significant advancement in BMI versatility, supporting the capability of a modular BMI system to accommodate multiple high priority effectors with little to no modifications to the rest of the system, reducing training time while maximizing multi-functionality.

II. Methods

A. Participant

The participant was a 27-year old man with tetraplegia from chronic C5 ASIA A spinal cord injury, who was enrolled in a clinical trial to decode hand/arm movements from his motor cortex (NCT01997125, Date: November 22, 2013). The trial was approved by The Ohio State University IRB (Columbus, OH) under an FDA Investigational Device Exemption. Four years prior to data collection for this report, the participant had a Utah microelectrode array (Blackrock Microsystems, Salt Lake, UT) implanted into the hand area of his dominant, left motor cortex as described in [10]. He provided written consent prior to study enrollment and gave

*The manuscript was submitted for review on 4/19/19. Research was supported by The Ohio State University, Blackrock Microsystems, Battelle Memorial Institute, and Ford Motor Company.

C. Dunlap, I. Burkhart, K. Eipel & M. Bockbrader are with The Ohio State University, Columbus, OH, USA. (marciebockbrader@gmail.com; phone: 614-293-3433).

L. Bird & F. Solzbacher are with the University of Utah, Salt Lake, UT, USA. L. Bird, F. Solzbacher, R. Franklin, & M. Gerhardt are with Blackrock Microsystems, Salt Lake, UT, USA. F. Solzbacher has financial interest in Blackrock Microsystems, which develops and commercializes neural interface and neuroscience research tools for clinical applications.

N. Annetta, C. Colachis, D. Friedenberg, P. Ganzer, & G. Sharma are with Battelle Memorial Institute, Columbus, OH, USA.

A. Ravindran (Palo Alto, CA, USA) and A. Hassani (Dearborn, MI, USA) are with the Research and Advanced Engineering Group of Ford Motor Company. D. Filev is Henry Ford Technical Fellow at Ford Motor Company, Dearborn, MI, USA.

permission for photographs and videos. Initial module connectivity and troubleshooting occurred on post-implant days 1574, 1609, 1616, and 1623. Testing sessions occurred on post-implant days 1630, 1665, 1672, 1679, 1686, 1693, 1700, 1721, 1728, 1730, and 1798.

B. *Hybrid System Overview*

The hybrid BMI for vehicle control consisted of four modules (Fig. 1): 1) a neural data acquisition system, 2) a neural signal processing and decoding workstation, 3) Python API to generate high level command signals from decoder values, and 4) CARLA simulation of vehicle control systems (VCS). Modules 1 and 2 are components of the NeuroLife® hand grasp system (Battelle Memorial Institute, Columbus, OH). Neural data from the participant's primary motor cortex were acquired through an implanted 96-channel intracortical microelectrode array and NeuroPort® interface (Blackrock Microsystems). Data was passed via Ethernet to a workstation running MATLAB-based decoding algorithms (The MathWorks, Inc., Natick, MA). Support vector machine (SVM) learning algorithms (LIBSVM) were used to classify neural data into hand/forearm movements (supination, pronation, hand open, hand closed). These movements were selected by the user for their intuitiveness as driving controls. Decoded hand movements were displayed to the user as movements of a hand animation (Fig. 1b). During Sessions 1-2, the hybrid system also utilized Estim as described in [10, 12, 16] to provide the user with limb movement feedback based on his motor intent. However, the participant reported arm movement to be distracting, Estim was discontinued, and his grip was stabilized on subsequent sessions (as in Fig. 1b).

To interface with the VCS, SVM decoder values were passed every 100ms via Ethernet to a laptop (Alienware 15 R2, Graphics Amplifier, GeForce GTX 1080Ti 11GB) running Python 3.6 (Python Software Foundation, python.org) and CARLA v.0.8.4 (http://carla.org/).

C. *Brain Data Decoding Algorithm and Training*

Neural data were sampled at 30kHz, digitized, and binned into 100ms segments for processing and discrete wavelet decomposition[10]. Standardized wavelet coefficients in the multiunit frequency band (~234-3750Hz) from *db4* wavelet scales 3-6 were used as neural features for an SVM model with 4 classes. Coefficients across scales were averaged per channel, smoothed with a 1-second boxcar filter, then used as a 1x96 input vector every 100ms to the SVM for model training and subsequent real-time motor intent classification.

A new classifier was trained each session, using up to 8 training blocks. During each block, the participant was presented with a visual cue (via hand animation) to rest or think of performing one of four hand/forearm movements (supination, pronation, hand open, hand closed). Each training block consisted of three cues of each type presented in random order for 3-4s with 7-8s (sessions 1-7) or 5-6s (sessions 8-11) of rest between cues. During the first block of training, scripted feedback was provided with each cue. In all subsequent blocks, feedback was given based on decoder outputs, which were generated based on a probability threshold for each movement class. Decoders were trained iteratively, using the three most recent blocks, until the user was satisfied with performance. Then, decoder parameters were locked and used for all subsequent driving tasks. Decoder training occurred during the first 20-30 minutes of each 3-hour experimental session.

D. *Python API*

A custom API mapped four-bit SVM movement decoder outputs to 4 possible simulated manual key presses in CARLA: Hand open, hand close, supination, and pronation were mapped to acceleration, deceleration, right turn, and left turn, respectively. The four-bit structure allowed for the potential to send multiple simultaneous commands to the vehicle, e.g., turning while braking; however, we constrained the BMI decoder to one movement class predicted per 100ms time bin to simplify training for this demonstration.

E. *Interface Optimization*

Several parameters of the BMI-VCS, including steering sensitivity, throttle, and brake, could range from stiff (0) to responsive (1). During initial sessions, the BMI-VCS used constant steering sensitivity (0.2), throttle (1.0) and brake (1.0) parameters. Parameters were adjusted across sessions based on the user's preference and sense of driving control.

An *exponential steering function* was implemented (Session 1) to enhance steering sensitivity at the lowest forward and reverse speeds and reduce sensitivity at higher

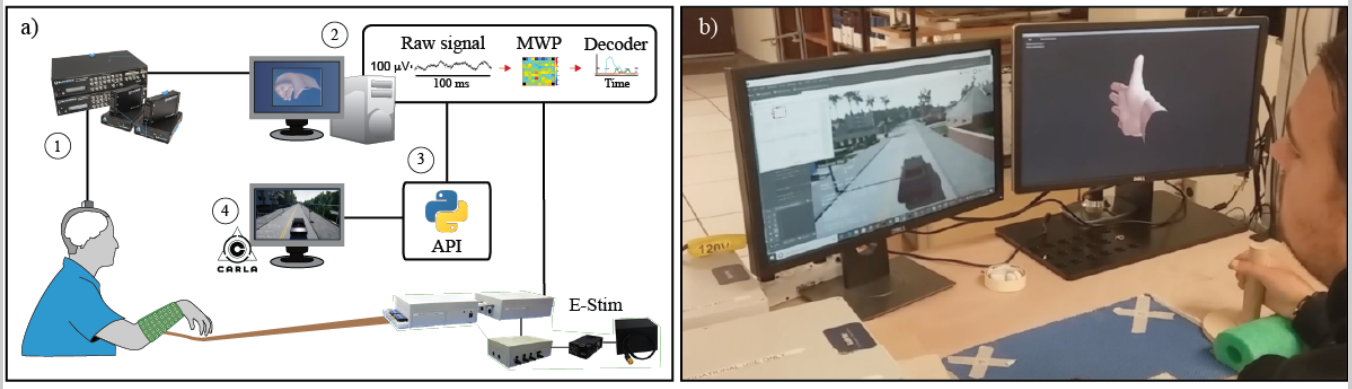

Fig. 1 Brain-machine interface – vehicle control system. a) Diagram of the hybrid system consisting of (1) Utah array and NeuroPort® data acquisition system, (2) signal processing and decoding workstation with neuromuscular electrical stimulator (Estim), (3) custom Python API to generate control signals from decoder values, and (4) CARLA driving simulator. b) Vehicle accelerates (at left) while user thinks about opening his hand (feedback animation at right) during real-time CARLA map navigation using the hybrid system.

speeds. This function was dependent on CARLA's built in *speed* measurement (which could be positive or negative and had arbitrary units):

$$\text{Steering Sensitivity} = \frac{3*(35-abs(speed))^{1.5}}{2000}. \quad (1)$$

A discretized throttle velocity scheme similar to *cruise control* was introduced (Session 2) to help the user maintain vehicle speed. Levels were set based on user preference and consisted of two reverse, one static, and five forward speeds:

$$\text{Cruise control speeds} = [-10, -5, 0, 4, 8, 15, 20, 25]. \quad (2)$$

To incrementally increase (decrease) cruise velocity, the participant transitioned from a rest to a hand open (hand closed) state. Throttle was applied if under the desired speed value, and brake applied if over. A sustained hand close or hand open decoder activation took priority over the cruise settings for as long as the decoder was above threshold. To rapidly decrease speed, *emergency braking* was implemented (Session 3) such that the vehicle stopped when the hand close decoder was activated twice within a 1.5sec sliding window.

The steering function was adjusted (Sessions 2-5) to:

$$\text{Steering Sensitivity} = \frac{3*(30-abs(speed))^{2}}{2000}. \quad (3)$$

To maximize decoder accuracy and minimize reaction time and steering overcorrection (Sessions 4-11), the *pre-SVM boxcar window* was systematically varied (between 0.5-1s) during model training and/or driving. The participant found that he preferred the boxcar width to be 1sec during training and 0.6sec during driving.

Additional adjustments were made (Sessions 6-9) to add a *stepwise exponential steering function* and optimize *cruise control* levels for enhanced steering stability at high forward speeds and to improve parallel parking performance:

$$\text{Steering Sensitivity} = \begin{cases} \frac{(30-abs(speed))^{2}}{2000} & if\ speed \le 4 \\ \frac{9*(30-abs(speed))^{2}}{50000} & if\ speed > 4. \end{cases} \quad (4)$$

Cruise control levels =[-7, -2, 0, 4, 8, 15, 20, 25].

A final cruise control adjustment was made (Sessions 10-11) to improve vehicle control during parallel parking:

$$\text{Cruise control levels} = [-5, -2, 0, 4, 8, 15, 20, 25]. \quad (5)$$

F. CARLA Simulator, Navigation Tasks, and Scoring

Six city driving tasks (Fig. 3) and one parallel parking task were created for this study. Tasks ranged from simple (Tasks 1 and 5) to complex (Task 6) based on number of turns and course distance. All CARLA simulations were performed using a third person perspective camera that was positioned above and behind the vehicle. A miniature map with the path for the current task was also shown. For simplicity, the participant was instructed to ignore stop signs and traffic lights. Pedestrians and other vehicles were removed, and weather was kept constant for all tasks. Driving checkpoints ensured that the expected path was taken.

Task performance was scored on metrics calculated within Python, including: whether a task was complete (i.e., the vehicle reached a target spatial location on the map), duration to complete the task (beginning with onset of forward motion and continuing until the vehicle passed a desired checkpoint), distance traveled during the task (sum of frame to frame changes in car's x,y,z coordinates), distance traveled off-road (>50% of car was off of road), number of times the car traveled off-road, distance traveled at least 50% out-of-lane, number of times out-of-lane, velocity (distance traveled/time), proportion of distance traveled out-of-lane (distance out-of-lane/total distance), proportion of distance traveled off-road (distance off-road/total distance), and distance traveled without deviations from road (total distance/times off-road +1). Parallel parking performance was evaluated qualitatively as either complete or incomplete.

G. Remote Control Model Car

To demonstrate feasibility of continuous, remote BMI control of a physical vehicle, we used previously saved decoder outputs to drive a remote control (RC) 1:10 scale Ford GT (Model 83056-4, TQi radio system, & Link wireless module; TRAXXAS, McKinney, TX) through a Python API. Driving controls were kept the same as in the simulation with the exception of scaled down velocity and constant steering sensitivity, as the offline driving trial occurred indoors.

H. Statistics

χ^2 tests were used to evaluate for significant differences in completion rate, proportion of distance traveled out of lane, and proportion of distance traveled off-road between CARLA maps. ANOVA (F-statistic) was used to evaluate for significant differences in completion time, distance traveled, and number of off road or lane deviation events between different CARLA maps. General linear models were fit to estimate significant predictors of velocity data. All statistics were completed in R (version 3.5.3, Vienna, Austria) using packages dplyr, data.table, car, and multcomp.

45 pt
0.625 in
15.9 mm

III. Results

The participant successfully completed all six CARLA routes, a parallel parking task, and offline, remote control of a model car using the BMI. Fig. 2 shows sample decoder activation patterns during task performance for four completed trials. Fig. 3 shows routes and metrics for the six navigation tasks. Fig. 4 shows how the offline, RC car path mapped to online BMI control of the driving simulator.

Across the six tasks, completion rate varied by session (Fig. 5a), $\chi^2(10)=24.716$, $p<0.006$, with a significant linear increase in completion rate as control commands were refined over time, $\chi^2(1)=5.438$, $p<0.02$). The completion rate also differed significantly between CARLA task maps, $\chi^2(5)=14.551$, $p<0.012$, with the most complicated route (Task 6) having the lowest completion rate.

A. Task-Specific Effects on Completion Time and Distance

Completion time and distance traveled differed significantly between tasks, $F(5,39)=17.55$, $p<0.0001$ and $F(5,39)=219.50$, $p<0.0001$, respectively, corresponding to differences in path length and complexity (Fig. 3). Post-hoc Tukey contrasts (Fig. 5b) revealed that Task 1 was completed significantly faster than Tasks 2 ($p<0.044$), 3 ($p<0.002$), and 6 ($p<0.001$); Task 4 was completed significantly faster than Task 6 ($p<0.004$); and Task 5 was completed significantly faster than Tasks 2 ($p<0.001$), 3 ($p<0.001$), 4 ($p<0.050$), and

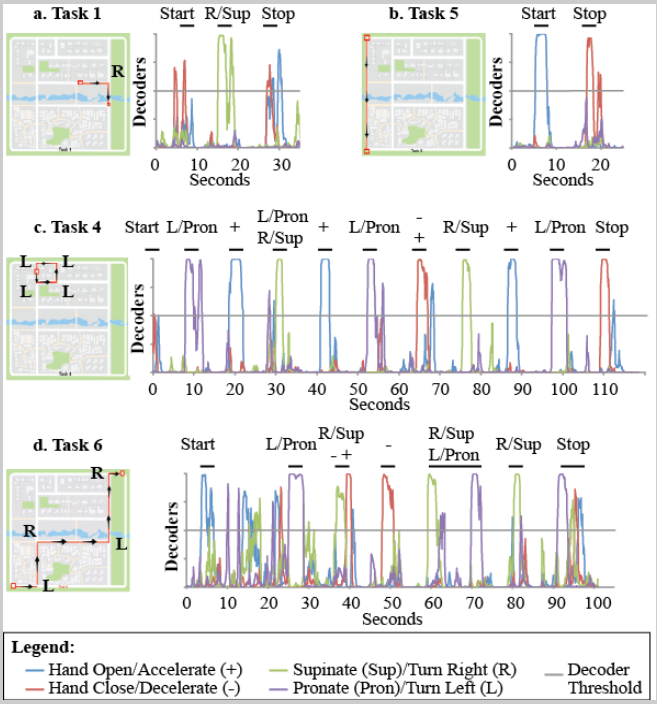

Fig. 2 Decoder activation patterns during four completed tasks from Session 5. The horizontal line indicates threshold for decoder activation. a) In Task 1, the user activated hand open to start, supinated to turn right, then activated hand close to stop. b) Task 5 was a long straight course that the user completed quickly. c) During Task 4, the user needed to make 4 left turns in succession. Intermittent steering corrections and acceleration/deceleration were also observed. d) Task 6 was the longest, most complicated course, involving alternating left and right turns. Steering overcorrections were noted throughout the course. This trial was the first complete Task 6 run.

6 ($p<0.001$). Distance traveled (Fig. 5c) differed significantly ($p<0.001$) between all pairwise contrasts except for Tasks 3-4, Tasks 3-5, and Tasks 4-5.

B. *Off-Road and Out-of-Lane Deviations*

The number of off-road events (vehicle >50% off-road) and distance traveled off-road did not differ between tasks. However, when off-road distance was normalized against total distance traveled (Fig. 5d), the vehicle spent proportionally less time out-of-lane on Task 6 compared to other tasks, $\chi^2(5)=29.641$, $p<0.0001$.

Number of lane-deviation events (vehicle >50% outside of lane) differed significantly between tasks $F(5,39)=9.232$, $p<0.0001$. Post-hoc Tukey contrasts revealed significantly more lane excursions on Task 6 than Tasks 1 ($p<0.001$), 2 ($p<0.043$), 4 ($p<0.012$), and 5 ($p<0.001$). There were also significantly fewer lane excursions on Task 5 compared to 3 ($p<0.045$). Distance traveled (>50%) outside of the lane differed significantly between tasks, $F(5,39)=6.515$, $p<0.0002$, with significantly more lane deviations for Task 6 compared to all other tasks (Tasks 2 and 3 at $p<0.001$, Tasks 1, 4 and 5 at $p<0.001$). However, when out-of-lane distance was normalized against total distance traveled, the vehicle spent proportionally less time out-of-lane on Task 6 compared to other tasks, $\chi^2(5)=29.641$, $p<0.0001$.

C. *Velocity*

Fig. 5e shows Velocity plotted across testing day, task type and whether the course was completed or incomplete. There was a main effect of both task ($F(5,71)=10.702$, $p<0.0001$) and trial completion ($F(1,71)=20.997$, $p<0.0001$) on velocity achieved by the CARLA vehicle. Velocity was significantly faster on completed trials than incomplete trials ($V_{completed}=5.1\pm3.8$ and $V_{incomplete}=2.0\pm1.3$). Post-hoc tests revealed that velocity was fastest for Task 5 ($t(76)=5.970$, $p<0.0001$), which was a straight course, and Task 6 ($t(76)=2.294$, $p<0.025$), which also had long straight sections. There was no significant practice effect on velocity after accounting for task type and course completeness.

D. *Contribution of Decoder Performance to Velocity*

Fig. 5f shows individual movement accuracy, sensitivity, and specificity of decoders during sessions with the highest (max) and lowest (min) overall decoder accuracy (calculated per [10] from the validation block of training). Overall accuracy represented the number of predictions that correctly matched the cue across movement classes. While accuracy (correct decoder identification of cues to move and rest) and specificity (correct identification of non-target cues) were reliably high across movements and days, sensitivity (correctly identified and sustained target cues) was more

	Task 1	Task 2	Task 3	Task 4	Task 5	Task 6	All
CARLA Map							
Completed attempts	**10**	**6**	**5**	**5**	**13**	**6**	**45**
Time (sec)***	68.6 (40.4)	115.2 (24.5)	135.9 (24.5)	90.2 (24.5)	43.6 (30.8)	161.4 (10.6)	89.8 (50.4)
Total distance (game units)***	179.0 (27.6)	396.4 (29.8)	297.7 (46.4)	268.8 (43.8)	307.1 (23.3)	683.6 (23.1)	335.4 (156.0)
Velocity (game units/sec)***	3.1 (1.0)	3.5 (0.6)	2.2 (0.3)	3.1 (0.4)	9.5 (4.6)	4.3 (0.3)	5.1 (3.8)
Off road events	1.1 (0.9)	1.8 (1.7)	2.0 (2.8)	1.4 (1.7)	0.8 (1.2)	0.8 (0.8)	1.2 (1.5)
Distance off road (game units)	7.6 (5.7)	15.5 (13.3)	20.0 (33.8)	9.3 (10.2)	16.8 (32.6)	4.6 (4.9)	12.5 (21.5)
Distance off road/Total (%)***	4.6% (3.7%)	4.0% (3.6%)	5.8% (9.2%)	3.2% (3.3%)	4.9% (9.4%)	0.7% (0.8%)	4.1% (6.3%)
Lane deviation events***	2.3 (1.5)	4.5 (4.0)	5.0 (3.2)	3.6 (2.4)	1.2 (1.5)	8.7 (2.3)	3.6 (3.3)
Distance outside lane (game units)***	42.8 (29.7)	48.8 (56.4)	55.1 (34.0)	32.1 (34.8)	58.4 (79.1)	228.2 (137.8)	73.0 (92.1)
Distance outside lane/Total (%)***	23.5% (16.7%)	12.2% (14.0%)	18.2% (10.0%)	12.2% (14.0%)	17.8% (23.6%)	33.3% (19.7%)	19.8% (18.6%)
Total attempts	**13**	**11**	**9**	**7**	**16**	**22**	**78**
Success rate**	77%	55%	56%	71%	81%	27%	58%

Values differed significantly between tasks **p<0.01, ***p<0.001

Fig. 3 Performance on CARLA driving simulator routes. Mean (standard deviation) time, distance, velocity and route deviation errors (>50% off road vs. >50% out of lane) for completed CARLA task attempts. Task 6 required many more attempts than simpler tasks to achieve our goal of 5-6 completions.

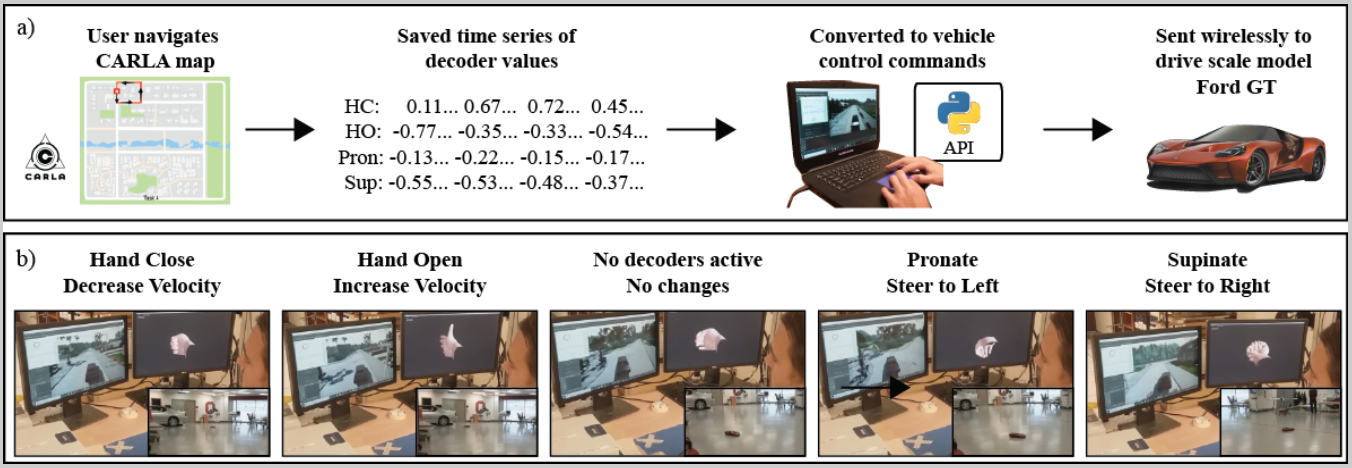

Fig. 4 Remote controlled car. a) Neural data acquired during CARLA simulation consisted of a time series of 4 decoder values every 100ms. The user drove the CARLA simulator by imagining movements of his paralyzed right arm (HC: hand close, HO: hand open, Pron: pronation, Sup: supination). Decoder values were saved, converted offline to velocity and steering control commands via a Python API, then sent wirelessly to a 1:10 scale remote controlled Ford GT. b) Sequential images obtained from videos recorded during navigation of Task 4 (counterclockwise loop) showing real-time BMI control of CARLA simulator, animated hand feedback corresponding to decoder activation, and position of Ford GT (inset) that was controlled offline using the time series of decoded brain signals.

variable. Fig. 5g shows that decoder sensitivity for the hand open movement (used to accelerate the vehicle) was significantly correlated with average velocity achieved per session (range: approx. 2-8 game units/sec) across all task attempts (R^2=0.46).

E. Effect of Steering and Velocity Control Adjustments

Our participant felt subjectively more in control of the CARLA vehicle after implementing *cruise control* (2) and a *stepwise, exponential steering function* (4) to improve turning sensitivity. Fig. 5h shows that quantitative analysis of performance metrics supported his belief. When metrics were normalized against performance achieved using sensitive steering and cruise control, it became clear that course completion (success rate), velocity achieved, and proportion of off-road events were worse on trials attempted without these steering and velocity control optimizations.

F. Parallel Parking

On Sessions 4, 6, and 8, the participant performed parallel parking on CARLA maps. To do this, he pulled up to a landmark (e.g., a low fence), reversed while turning, and then pulled forward while turning in the opposite direction. Fig. 6 shows a representative, successful parallel parking attempt from Session 8. Adjusting steering sensitivity (4) and reverse throttle speed (5) improved the participant's ability to maneuver and parallel park without hitting objects.

G. Offline BMI-RC Car Demonstration

In an offline session (Fig. 4), decoder values obtained during successful completion of Task 4 during Session 6 were used to drive a 1:10 scale remote control Ford GT. Decoder outputs, processed in the same four bits, were used to manipulate one output signal for steering and one for acceleration. In this way, the user provided high-level, shared control for the car through BMI signals obtained while he thought about driving. To achieve incremental increases in speed, the active cruise setting was used to vary the duty cycle of a pulse width modulated (PWM) output. Because turning sensitivity was eliminated in offline control, the steering signal duty cycle was kept constant. The output signals were subsequently low pass filtered and used as input to the car's wireless control transmitter. Due to space limitations for car operation, decoder outputs were processed every 65ms instead of 100ms, in effect reproducing the CARLA map for Task 4 (counter-clockwise loop) at a smaller scale suitable for the indoor course.

IV. Discussion

In this proof of concept study, we have demonstrated how the NeuroPort recording and NeuroLife decoding modules of a hand-grasp BMI can be repurposed to provide real-time, accurate control signals for driving. By connecting neural interface and machine learning components with a flexible API for end-effectors, neural activity associated with upper limb motor intent was captured, classified, and remapped in real time from Estim commands for grasp, to velocity and steering controls for driving. In this demonstration, a Python API was used to translate SVM classifier outputs of the user's motor intent into virtual keystrokes of the driving simulator, allowing the user to accelerate, decelerate, turn, and parallel park as he navigated CARLA tasks. This mapping was facilitated by the user's association between hand/forearm states (e.g., supination) and vehicle controls (turning right). In order to optimize high-level control of the driving simulator, a trial-and-error method was used to adjust the nonlinear transformation of decoder outputs to VCS states based on user feedback. The API and nonlinear transformation scheme could potentially be extended further to control other devices (e.g., an exoskeleton) substituted to meet a user's particular need.

The ability of the BMI-VCS hybrid to control a simulated vehicle in city driving scenarios demonstrates the potential of BMI to provide real-time, high-level, shared control of a vehicle where certain lower-level driving functions are automated. Similar proposals have been made for EEG-based power wheelchair controls [6, 7]; note, however, that EEG-

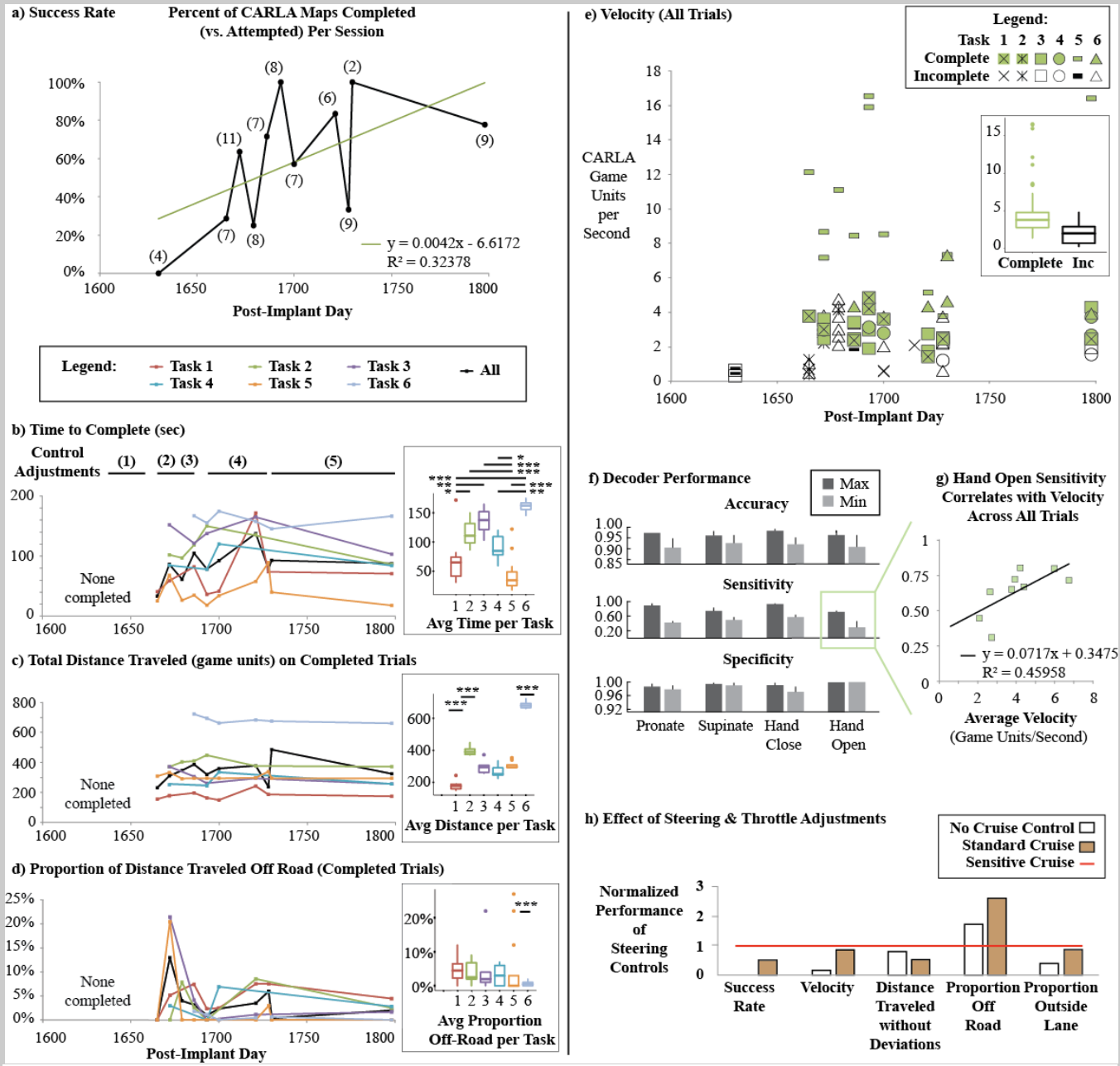

Fig. 5 CARLA Performance Using the BMI. a) Success rate, or percent of all CARLA maps attempted that were completed, improved linearly across sessions. X-axis is post-implant day. b) Time to complete courses varied by task and also showed some variability as steering and throttle controls were adjusted (per equations (1) –(5)). X-axis is post-implant day. c) Distance traveled (on completed courses) also varied by task, but remained constant within each task across time. d) Proportion of distance traveled off-road differed by task and varied with steering and throttle adjustments. e) Velocity achieved was greater in completed trials than incomplete trials and for tasks with long straight sections (Tasks 5 and 6). f) Individual movement accuracy, sensitivity and specificity for sessions with highest (max) and lowest (min) overall accuracy are shown. Values were similar to those observed with this participant in prior studies. [10, 16] Hand open sensitivity was positively correlated with average vehicle velocity achieved per session. h) Performance without cruise control and with standard cruise was normalized against performance with sensitive steering and cruise control for comparison. Without cruise control, the participant struggled to complete CARLA tasks and could not maintain his driving velocity. After adding cruise control (2), he improved his completion rate and velocity, but went off road frequently due to an escalating cycle of steering overcorrections. After implementing a stepwise, exponential steering function along with cruise control (4), the participant was able to successfully complete maps, maintain driving velocity, and improve proportion of distance traveled without going off road. *Significance level of post-hoc contrasts: *p<0.05, **p<0.01, ***p<0.001*

45 pt
0.625 in
15.9 mm

based systems are limited by their lower sampling rate, slower response time, and number of operations that can be classified simultaneously. The BMI-VCS hybrid system also differs from autonomous vehicles that rely on sophisticated sensors, perception and decision-making systems for path planning and following; here, the human BMI user acts as the sensor and high-level decision-maker based on his/her own perceptions, e.g., to avoid collisions or to time a turn

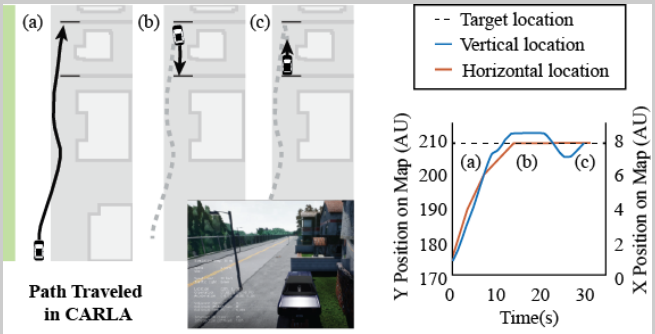

Fig. 6 Parallel parking example from Session 8. Overhead view of the path traveled over time (a)-(c), screenshot of the final vehicle position in (c), and plot of change in XY position while parking.

appropriately. This type of assistive device would enable many individuals with restricted motor control but intact vision and cognition to regain independence for driving, which is expected to significantly enhance quality of life.

In addition to successfully driving CARLA routes under BMI control, we have shown proof of concept that BMI data obtained while the user imagined navigating a route (Task 4) can be successfully used offline to remotely control a vehicle through the same route. However, real-time BMI control of the RC vehicle remains to be shown. Use of BMI for navigation in a real environment can pose additional challenges in comparison to a simulation, an example being a reliable communication system between the BMI-VCS and the RC vehicle. The scope of the navigation environment along with the view of the vehicle as well as the vehicle's path of motion might significantly impact the subject's perception and mental strategy for fine control of specific movements. The need for more flexible control systems that allow execution of two commands simultaneously along with the amount of workload or fatigue experienced by the subject are some other barriers of online BMI-RC control that may need further investigation.

Driving a manned wheelchair or vehicle is a complicated and challenging endeavor, with many risks and serious consequences in the event of failure. Any feedback-control system must adhere to functional safety standards, whereby the controller must have sufficient response time, fault tolerance and fault mitigation methods. In the case of the CARLA simulator, we observed that at least optimization of steering and throttle control were required to minimize steering over-correction and adjust steering sensitivity to speed. A suggested approach for further improving control robustness would be to incorporate intermediary steps beyond the CARLA inputs for acceleration, deceleration, right turn and left turn. This would allow more resolution in command input, as well as dampen the behavior to reduce BMI-control overshoot.

Another feedback-control problem could arise from the current chase camera view of the vehicle in the CARLA simulator. This third person perspective allows the participant to clearly view the entire vehicle along with the closest lane boundaries surrounding the vehicle and control the steering accordingly to maintain lanes. A dashboard camera view or a driver's view of the vehicle may elicit a different behavior of steering control, especially during turns. This might require further optimizations of steering and throttle control that may affect off-road and out-of-lane deviations.

It is theorized that feedback-control performance could also be improved by shortening the 100ms window for neural sampling and decoder processing to 5ms to reduce lag time. Using a 100ms window, the SVM decoders required about 600-800ms (6-8 cycles) to generate accurate classifications, introducing a response delay based on system architecture. While it is currently unknown what the optimal window width is to simultaneously maximize accuracy and response time or how many decoder cycles are required to reliably capture neural signatures of motor intent, reducing the sample time should in general minimize stopping time and enhance vehicle maneuverability. In addition, a transition away from SVM decoders to another machine learning approach is likely necessary to optimize tradeoffs between decoder accuracy, multi-functionality, false positive rate, and response time. We have recently shown that a deep neural network decoder outperforms SVM and other algorithms when decoding arm and hand movements [17, 18]. Future work should investigate whether a deep neural network improves feedback control for driving, especially in combination with proportional control of turns – a feature desired by the user.

In addition, future work will expand on the relatively simplistic analysis of driving simulator performance reported here and integrate CARLA's AI metrics for manual performance. For example, our results indicate that longer courses with more turns take longer to traverse and are harder to complete. Taking the next step and comparing the BMI-enabled path against an optimal path, i.e., how much of the distance traveled was directed toward the goal, is a better estimation of performance because it provides insights into where and why errors occur. This provides a target for future optimizations, where greater inferences could be made by also incorporating lateral offset, lateral offset velocity and rotational velocity into the analytics model. Future work will also need to test BMI control on more realistic simulator maps with agents like pedestrians, vehicles, traffic signals as well as factors like multiple lanes and traffic. This would allow comparison to metrics used in the standard driving literature, e.g., time to collision (TTC) and mean lane deviation (MLD), as well as assessment of whether the user can maintain BMI control with divided attention and manage unexpected environmental events. Finally, real-time remote control of unmanned vehicles or other remotely controlled effector devices will need to be safely demonstrated prior to moving to real-time BMI control of manned vehicles.

As device manufacturers and investigators are solving some of the hardware problems [19] to make an intracortical BMI portable, we are edging ever closer to the day when an intracortical BMI controller operates as an assistive device not only outside of the lab, but inside a car. It turns out that many of the optimization processes required for precision control of a speeding vehicle on a complicated course are the innovations needed to use a BMI in the home for activities of daily living. For example, they both require secure, private communication between the BMI and (a potentially remotely controlled) effector. Both also require stable, reliable, and robust operation regardless of potential electromagnetic noise

in the environment. Finally, to minimize accidents, both require feedback control systems that minimize lag time, maintain their accuracy without requiring frequent recalibration, and work effectively with an intuitive interface that allows for multi-tasking. Solutions that can address these challenges will ultimately provide technology that can be deployed in multiple ways to improve the lives of individuals living with impairment.

V. Conclusion

By adapting a BMI for hand grasp into a hybrid BMI-VCS for driving control, we have shown that advancing technology for the control of one end effector may carry over quite readily to improved control of other effectors. This versatility is important for other potential applications, such as the eventual translation of BMI into patients' homes, not only because prospective BMI users prioritize multi-functionality [13, 14], but also because devices are more likely to be abandoned when the users' needs or priorities change [20]. Conceptualizing of BMI technology modularly, optimizing components in a way that make them downwards compatible, and treating end-effectors as shared control devices will maximize the flexibility and usefulness of BMI systems outside the research lab. For example, a single BMI system could be integrated with smart home technology, mobility devices such as a wheelchair, and a device to restore or replace arm and hand function. Upon chronic changes in the user's abilities or needs, the effectors could be replaced or upgraded. Such considerations are of particular importance for those with progressive neuromuscular disorders or those who regain functional ability after traumatic injury.

Acknowledgment

The authors thank Ford for graduate research assistant support, and Neil Austin for assistance with figures.

References

[1] L. R. Hochberg, D. Bacher, B. Jarosiewicz, N. Y. Masse, J. D. Simeral, J. Vogel, *et al.*, "Reach and grasp by people with tetraplegia using a neurally controlled robotic arm," *Nature* vol. 485, pp. 372-375, 2012.

[2] J. L. Collinger, B. Wodlinger, J. E. Downey, W. Wang, E. C. Tyler-Kabara, D. J. Weber, *et al.*, "High-performance neuroprosthetic control by an individual with tetraplegia," *Lancet,* vol. 381, pp. 557-64, 2013.

[3] D. J. McFarland, D. J. Krusienski, W. A. Sarnacki, and J. R. Wolpaw, "Emulation of computer mouse control with a noninvasive brain–computer interface," *Journal of neural engineering,* vol. 5, p. 101, 2008.

[4] J. Simeral, S.-P. Kim, M. Black, J. Donoghue, and L. Hochberg, "Neural control of cursor trajectory and click by a human with tetraplegia 1000 days after implant of an intracortical microelectrode array," *Journal of neural engineering,* vol. 8, p. 025027, 2011.

[5] M. J. Vansteensel, E. G. M. Pels, M. G. Bleichner, M. P. Branco, T. Denison, Z. V. Freudenburg, *et al.*, "Fully Implanted Brain–Computer Interface in a Locked-In Patient with ALS," *New England Journal of Medicine,* vol. 375, pp. 2060-2066, 2016.

[6] T. Carlson and J. d. R. Millan, "Brain-controlled wheelchairs: a robotic architecture," *IEEE Robotics & Automation Magazine,* vol. 20, pp. 65-73, 2013.

[7] Á. Fernández-Rodríguez, F. Velasco-Álvarez, and R. Ron-Angevin, "Review of real brain-controlled wheelchairs," *Journal of neural engineering,* vol. 13, p. 061001, 2016.

[8] G. Pfurtscheller, G. R. Müller, J. Pfurtscheller, H. J. Gerner, and R. Rupp, "'Thought'–control of functional electrical stimulation to restore hand grasp in a patient with tetraplegia," *Neuroscience letters,* vol. 351, pp. 33-36, 2003.

[9] R. Rupp, M. Rohm, M. Schneiders, N. Weidner, V. Kaiser, A. Kreilinger, *et al.*, "Think2grasp-bci-controlled neuroprosthesis for the upper extremity," *Biomedical Engineering/Biomedizinische Technik,* 2013.

[10] C. E. Bouton, A. Shaikhouni, N. V. Annetta, M. Bockbrader, D. A. Friedenberg, D. M. Nielson, *et al.*, "Restoring cortical control of functional movement in a human with quadriplegia," *Nature,* vol. 533, pp. 247-50, 2016.

[11] A. B. Ajiboye, F. R. Willett, D. R. Young, W. D. Memberg, B. A. Murphy, J. P. Miller, *et al.*, "Restoration of reaching and grasping movements through brain-controlled muscle stimulation in a person with tetraplegia: a proof-of-concept demonstration," *Lancet,* vol. 389, pp. 1821-1830, 2017.

[12] M. Bockbrader, N. Annetta, D. A. Friedenberg, M. Schwemmer, N. Skomrock, S. C. Colachis IV, *et al.*, "Clinically significant gains in skillful grasp coordination by an individual with tetraplegia using an implanted brain-computer interface with forearm transcutaneous muscle stimulation," *Archives of Physical Medicine and Rehabilitation,* 2019.

[13] J. L. Collinger, M. L. Boninger, T. M. Bruns, K. Curley, W. Wang, and D. J. Weber, "Functional Priorities, Assistive Technology, and Brain-Computer Interfaces after Spinal Cord Injury," *J Rehabil Res Dev,* vol. 50, pp. 145-160, 2013.

[14] J. E. Huggins, A. A. Moinuddin, A. E. Chiodo, and P. A. Wren, "What would brain-computer interface users want: opinions and priorities of potential users with spinal cord injury," *Archives of physical medicine and rehabilitation,* vol. 96, pp. S38-S45. e5, 2015.

[15] A. Dosovitskiy, G. Ros, F. Codevilla, A. Lopez, and V. Koltun, "CARLA: An open urban driving simulator," vol. arXiv:1711.03938, 2017.

[16] N. Annetta, J. Friend, A. Schimmoeller, V. S. Buck, D. A. Friedenberg, C. E. Bouton, *et al.*, "A High Definition Non-invasive Neuromuscular Electrical Stimulation System for Cortical Control of Combinatorial Rotary Hand Movements in a Human with Tetraplegia," *IEEE Transactions on Biomedical Engineering,* 2018.

[17] M. Schwemmer, N. Skomrock, P. B. Sederberg, J. Ting, G. Sharma, M. Bockbrader, *et al.*, "Meeting brain-computer interface user performance expectations using a deep neural network decoding framework," *Nature Medicine,* p. in press, 2018.

[18] N. D. Skomrock, M. A. Schwemmer, J. E. Ting, H. R. Trivedi, G. Sharma, M. A. Bockbrader, *et al.*, "A Characterization of Brain-Computer Interface Performance Trade-Offs Using Support Vector Machines and Deep Neural Networks to Decode Movement Intent," *Frontiers in Neuroscience,* vol. 12, 2018-October-24 2018.

[19] J. Weiss, R. Gaunt, M. Boninger, R. Franklin, and J. Collinger, "Development of a portable intracortical BCI system," in *7th International BCI Meeting*, Asilomar, CA, 2018, pp. 131-2.

[20] B. Phillips and H. Zhao, "Predictors of assistive technology abandonment," *Assistive technology,* vol. 5, pp. 36-45, 1993.